THE OFFICIAL MAGAZINE OF THE OCEANOGRAPHY SOCIETY

Oceanography



DOI

http://dx.doi.org/10.5670/oceanog.2015.14

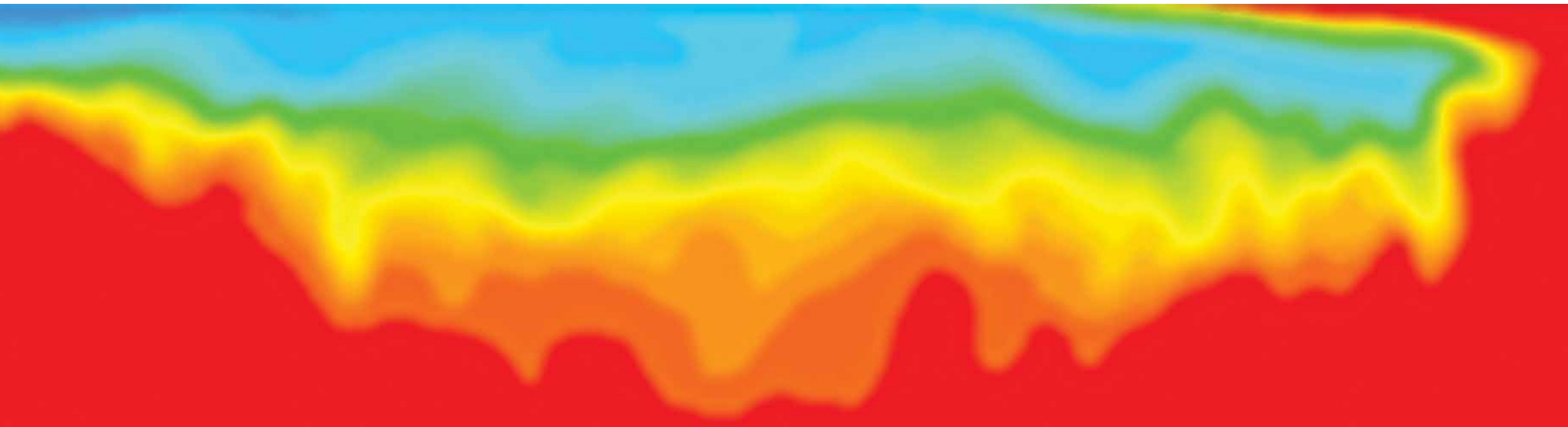

# Three-Dimensional Dynamics of Freshwater Lenses in the Ocean's Near-Surface Layer

By Alexander V. Soloviev,
Silvia Matt,
and Atsushi Fujimura

**ABSTRACT.** Convective rains in the Intertropical Convergence Zone produce lenses of freshened water on the ocean surface. Due to significant density differences between the freshened and saltier seawater, strong pressure gradients develop, resulting in lateral spreading of freshwater lenses in the form of gravity currents. Gravity currents inherently involve three-dimensional dynamics. As a type of organized structure, gravity currents may also interact with, and be shaped by, the ambient oceanic and atmospheric environment. Among the important environmental factors are background stratification and wind stress. Under certain conditions, a resonant interaction between a propagating freshwater lens and internal waves in the underlying halocline (the barrier layer) may develop, while interaction with the wind stress may produce an asymmetry in the freshwater lens and associated mixing. These two types of interactions working in concert may explain the series of sharp frontal interfaces observed in association with freshwater lenses during the Tropical Ocean Global Atmosphere Coupled Ocean Atmosphere Response Experiment (TOGA COARE). We conducted a series of numerical simulations using computational fluid dynamics tools. These numerical experiments were designed to elucidate the relationship between vertical and horizontal fluxes of salinity under various environmental conditions and the potential impact of these fluxes on the barrier layer and Aquarius and Soil Moisture and Ocean Salinity (SMOS) satellite image formations.

## INTRODUCTION

Buoyancy-driven surface currents, such as propagating rain-formed lenses or plumes (we use these terms interchangeably), are an important component of the tropical ocean environment in the Intertropical Convergence Zone (ITCZ; see, e.g., Wijesekera et al., 1999). These currents contribute to water mass exchange by horizontal advection and enhanced vertical mixing. As buoyancy-driven flows, they are a type of organized structure that resembles a classical gravity current. The water flow in the leading edge of the gravity current and trailing fluid contains a complex pattern of three-dimensional motions (Özgökmen et al., 2004). Gravity currents may also interact with ambient stratification in a resonant way, leading to fragmentation of the near-surface lens, and with the surface wind stress, resulting in lens asymmetry in structure and mixing (Simpson, 1987; Soloviev and Lukas, 1997; Matt et al., 2014). The patterns in gravity currents are inherently three dimensional.

Notably, the dynamics of the freshwater lenses produced by convective rains can be linked to larger-scale features (e.g., barrier layer and salinity fronts), thus influencing global-scale processes and contributing to the salinity field detected in the Aquarius and Soil Moisture and Ocean Salinity (SMOS) satellite footprints. The barrier layer (Lukas and Lindstrom, 1991) separates the well-mixed surface layer from the thermocline, which enhances the air-sea coupled response. A substantial amount of data on freshwater plumes was collected during the Tropical Ocean Global Atmosphere Coupled Ocean Atmosphere Response Experiment (TOGA COARE). Soloviev and Lukas (2014) summarize these materials. The NASA Salinity Processes in the Upper-ocean Regional Study (SPURS) obtained new and interesting data on freshwater plumes (e.g., Anderson and Riser, 2014; Asher et al., 2014). However, these data are still fragmentary; more details about freshwater plume dynamics are required before these subgrid-scale phenomena can be incorporated into global ocean circulation models and operational algorithms for sea surface salinity satellites.

Oceanic advection and mixing fundamentally affect the sea surface salinity signal sensed by the two satellites. Improved understanding of these processes is one of the SPURS goals (Farrar et al., 2014). In this paper, we apply computational fluid dynamics tools to investigate horizontal spreading and vertical mixing of the freshwater plumes produced by convective rains in the ITCZ. We then briefly explain the model setup and describe the computational experiments designed to illustrate the interaction of rain-formed plumes with their environments. The modeling results are compared with conceptual models developed during TOGA COARE.

## MODEL DESCRIPTION

Because the processes involved in the propagation and mixing associated with near-surface freshwater plumes are three dimensional, explicitly modeling their dynamics requires a high-resolution, nonhydrostatic three-dimensional modeling approach. Thus, to simulate the low-density plume, we implemented a computational fluid dynamics model with the numerical domain shown in Figure 1a, following Matt et al. (2014). Periodic boundary conditions are set on the walls along the tank direction. The boundary conditions at the bottom and the side walls of the numerical tank are

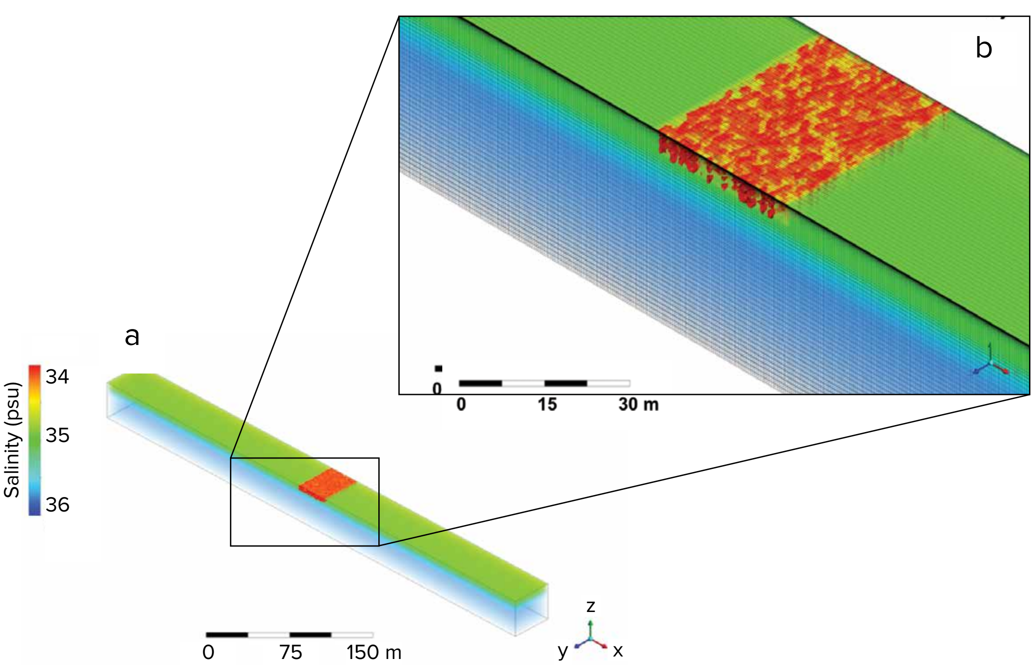


FIGURE 1. Numerical domain and model initialization (red color corresponds to lower salinity). (a) 500 m x 40 m x 40 m domain containing 3,120,000 cells. Δz = 1 cm (at the top). Δx = 50 cm, Δy = 1 m. (b) A close-up of the initial conditions showing the low salinity anomaly produced by convective rain at the top of the domain, with the halocline below.

specified as zero shear, and zero heat and salinity fluxes are set at the bottom, side walls, and top of the tank. We initialize the model with a rain cell (Figure 1a) simulating randomly distributed rainfall near the top of the domain (Figure 1b). Salinity stratification, for example, a halocline representing the barrier layer (Lukas and Lindstrom, 1991), can be added to the model during initialization, and wind stress can be applied at the top of the tank. We tested a number of wind stress and halocline parameter combinations.

In this article, depending on the case, we use either the LES WALE or DES model. More details on the numerical schemes and setup, including the WALE and DES formulations, can be found in Matt et al. (2011, 2014).

## NUMERICAL SIMULATIONS AND RESULTS

We conducted high-resolution numerical experiments on the dynamics of near-surface buoyant plumes in the presence of ambient stratification and wind

"These numerical experiments were designed to elucidate the relationship between vertical and horizontal fluxes of salinity under various environmental conditions and the potential impact of these fluxes on the barrier layer and Aquarius and Soil Moisture and Ocean Salinity (SMOS) satellite image formations."

stress. The following process studies were performed using the computational fluid dynamics model described in the previous section. Depending on the case, environmental conditions for the evolving buoyant plume are set either via initial conditions (salinity stratification) or as a boundary condition at the top of the domain (wind stress).

In this work, we used a large eddy simulation (LES) to model freshwater lens dynamics. Two LES algorithms were implemented: LES with Wall-Adapting Local Eddy-Viscosity (WALE) as a subgrid-scale model (Nicoud and Ducros, 1999) and a Hybrid LES-Detached Eddy Simulation (DES) (Strelets, 2001). Both models have advantages and disadvantages. WALE is optimized for rigid-lid boundary conditions (e.g., bottom and side walls in our simulations); however, it results in excessive surface drift velocity when wind stress is applied at the top of the numerical tank due to absence of surface waves. DES results in more realistic surface drift (Matt et al., 2011) but produces less realistic results near the rigid walls where the specified zero-shear boundary condition is applied.

### Freshwater Lens Propagating Under Calm Weather Conditions in Nonstratified and Stratified Environments

Figure 2 shows the spreading of a rain-formed plume in an unstratified environment, simulated using the LES WALE algorithm. The low-salinity lens was initialized in the near-surface layer as a salinity anomaly within a 5 m deep box with horizontal dimensions of 40 m × 40 m in the x and y directions. The initial salinity anomaly was randomly distributed at a 1.2 psu peak and 0.6 psu average level, well within the range of near-surface salinity anomalies observed in the western equatorial Pacific (Soloviev and Lukas, 2014).

As the plume evolved from its initial state (see Figure 1), randomly distributed rain signatures quickly merged into a continuous low-salinity plume. Figure 2a shows contour plots of the freshwater plume's velocity field at the surface and at 13 m depth after 2,500 s of simulation. The simulation was limited to 2,500 s because the spreading plume was approaching the domain's boundaries. The frontal edges of the plume spread with a speed of 0.14 m $s^{-1}$ along the tank. The modeled current velocities are of the same order of magnitude as observations (Wijesekera et al., 1999; Soloviev et al., 2002). The spreading plume induces velocity fluctuations of the order of 0.004 m $s^{-1}$ below the plume fronts at a 13 m depth. Because the initial density anomaly was in the center of the tank, the velocity pattern in this simulation was almost symmetrical with respect to the center of the tank. After 2,500 s of simulation, the freshwater lens significantly expanded horizontally but collapsed in the vertical direction, from 5 m to roughly 1 m thickness (Figure 2d). It is, however, necessary to remember that this simulation was performed for calm weather conditions.

The contour plot of the salinity gradient in Figure 2b reveals a streak-like structure in the fluid trailing behind the plume edge. The streaks are approximately aligned with the plume propagation direction but are intermittent. The cross-section contour plot of the vertical velocity shown in Figure 2c suggests that these structures have the form of rolls. The nature of these streaks in the ocean is still not completely clear; they may be of the same nature as Lesieur's (2008) streaks or Kuettner's (1971) atmospheric rolls. These coherent structures can be caused by vertical shear within the propagating plume. Note that Özgökmen et al. (2004) reproduced similar coherent structures in a three-dimensional numerical simulation of an overflow gravity current. The width of streaks is an order of magnitude larger than the thickness of the freshwater lens, and their length is two orders of magnitude larger than the thickness of the freshwater lens. These numbers are consistent with Lesieur's (2008) conceptual model.

With the addition of the halocline below the initial freshwater anomaly, further interaction was observed. In this experiment, we initialized the halocline with the linear salinity change of 4 psu between 6 m and 16 m water depth. This initialization resembles a halocline (barrier layer) reported by Vinayachandran et al. (2002) in the northern part of the Bay of Bengal.

Figure 3 shows contour plots of the velocity field on the surface and at 13 m depth after 2,500 s of simulation. In the case of no stratification, the propagating freshwater plume induced the circulation below its edge (Figure 2a). In the case of environmental stratification (halocline), plume propagation resulted in the excitation of internal waves in the underlying halocline and apparent modulation of the lens structure by these internal waves (Figure 3a). The internal waves excited in the barrier layer by the freshwater lens propagate somewhat ahead of the lens edge (Figure 3c).

Based on the laboratory results of Simpson (1987), Soloviev and Lukas (1997) hypothesized that the freshwater lens in the ocean's near-surface layer may interact with environmental stratification. A small thickness of the near-surface anomalies is favorable for the development of nonlinear interactions. These laboratory studies indicate that any density anomaly in the upper layer tends to spread horizontally. The leading edge of the gravity current along a boundary through a uniformly stratified medium can generate several different modes of internal waves.

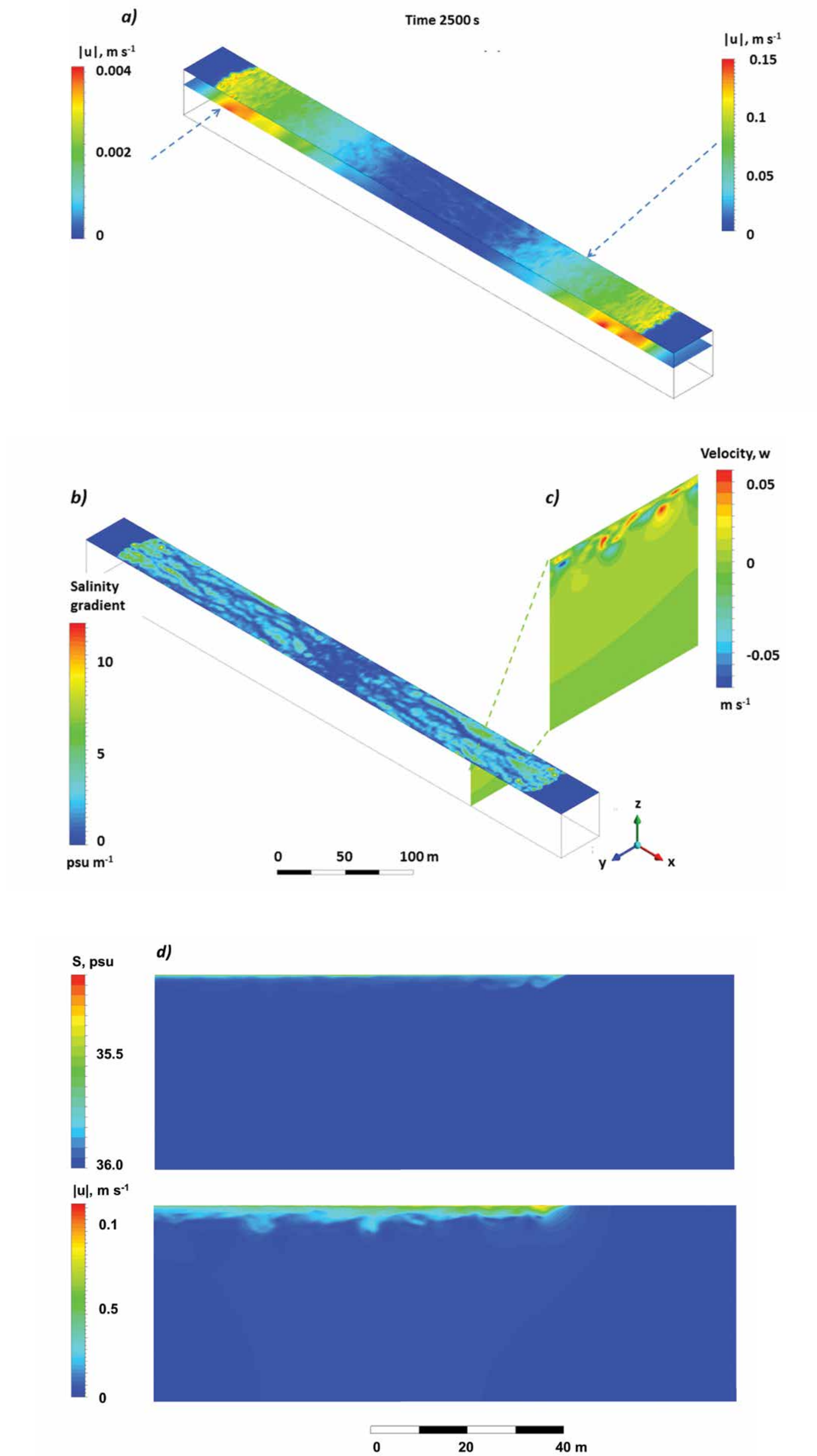


FIGURE 2. (a) The velocity magnitude field at the surface and at 13 m depth induced by the freshwater lens spreading from the initial position of the plume at the center of the domain into a non-stratified environment after 2,500 s of simulation. (b) Coherent structures seen in the magnitude of the salinity gradient on the top of the spreading freshwater plume. (c) Contour plot of the vertical velocity component reveals rolls inside the propagating plume. (d) Salinity and magnitude velocity contour plots near the plume edge (side view).

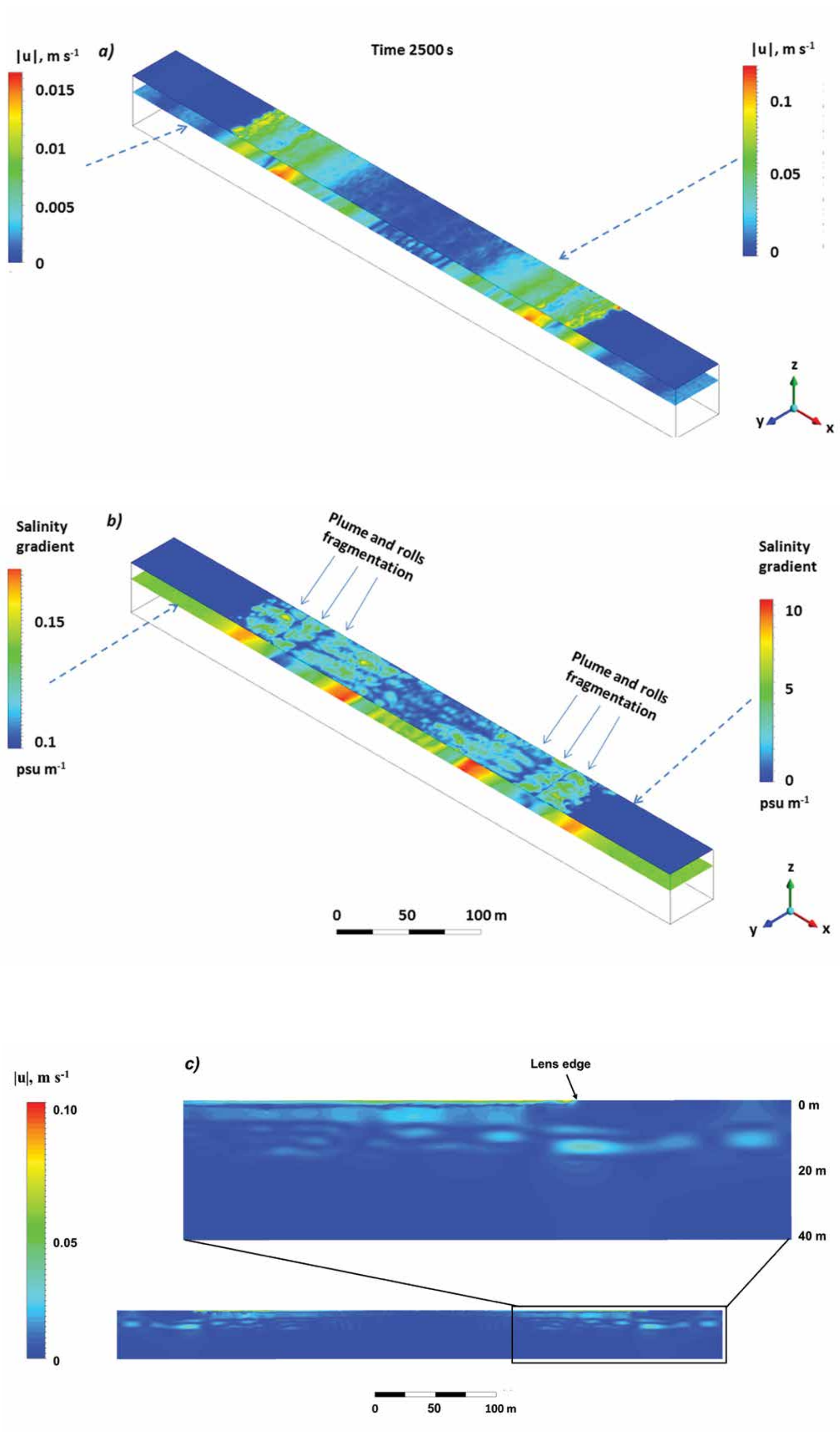


**FIGURE 3.** (a) The velocity magnitude field at the surface and at 13 m depth induced by the freshwater lens propagating above, and interacting with, the underlying halocline. (b) Fragmentation of the plume into bands due to resonant interaction with the underlying halocline. (c) Contour plots of the velocity magnitude (side view) showing generation of internal waves by the spreading lens. Note the internal waves propagating ahead of the lens edge.

According to the laboratory observation described by Simpson (1987), "These waves affected the form of the gravity current behind the head in a rhythmical manner. The fluid in the original head was cut off from the flow, which formed a second head. The process was repeated and later a third new front appeared…" However, this striking effect was observed only when the following conditions for the Froude number (*Fr*) and the fractional depth of the gravity current (*r*) were satisfied:

$$Fr = U/NH < 1/\pi \qquad (1)$$

and

$$r = h/H < 0.2 \qquad (2)$$

where $U$ is the speed of the gravity current, $h$ is the thickness of the gravity current, $H$ is the depth of the ocean, $N$ is the Brunt–Väisälä frequency of the stratified surroundings, and $\pi = 3.14$. This is a resonant type mechanism of interaction between the freshwater lens and the stratified environment.

In the case shown in Figure 3, $Fr = 0.08$ and $r = 0.05$; according to conditions (1) and (2), resonant interaction between the freshwater plume and the underlying halocline was expected. For the no-stratification case shown in Figure 2, there is no halocline ($Fr = \infty$), so no resonant interaction was possible.

The banding pattern on the surface (Figure 3a) can be interpreted as an indication of the plume fragmentation due to resonant interaction with the ambient stratification. Notably, this fragmentation interrupted the coherent rolls as well (Figure 3b).

### Interaction of Freshwater Plume with Wind Stress

Next, we investigated the case of a freshwater plume interacting with wind stress in a nonstratified environment. In order to produce a realistic aqueous viscous sublayer, a DES scheme was implemented. We applied wind stress at the top of the numerical tank and spun up the model for 500 s. The plume simulation was then initialized with a low-salinity plume, imitating randomly distributed rainfall similar to Figure 1 but with no stratification below the freshwater plume. We tested the three cases corresponding to wind speeds at 10 m height, $U_{10} = 0$ m s$^{-1}$, $U_{10} = 4.0$ m s$^{-1}$, and $U_{10} = 8.5$ m s$^{-1}$ (Figure 4). The plume structure showed a notable asymmetry relative to the wind direction when forced with wind stress. The asymmetry of the plume apparently increases with wind speed.

The plume asymmetry caused by wind stress is clearly seen in Figure 5, which shows two isosurfaces associated with the freshwater plume. Figure 6 shows evolution of the freshwater plume in time. Notably, mixing on the upwind side of the plume is more intense than on the downwind side of the plume.

The asymmetry of freshwater plumes relative to the wind speed direction was observed in the western equatorial Pacific during TOGA-COARE (Soloviev and Lukas, 1997; Soloviev et al., 2002). Soloviev and Lukas (1997) suggested that this asymmetry can be explained by the mechanism of Stommel's (1993) Overturning Gate, schematically shown in Figure 7. When the wind stress is directed toward lower density, gravitational instability may trigger Kelvin-Helmholtz instability and intensive vertical and cross-frontal mixing (Soloviev and Lukas, 1997). In the process of mixing, the interface may either reach the compensated state in density (when the temperature differences associated with the low-salinity lens are accounted for) or entirely disappear; in both cases, the interface is no longer prominent in the density field. When the wind stress is directed toward higher density, stable stratification increases due to lateral advection of less dense water, which inhibits mixing. Consequently, the downwind frontal interface "freezes" and can drift downwind until the wind substantially changes either in direction or speed with respect to the plume.

According to the criteria proposed by Soloviev et al. (2002), instability on the upwind edge of the plume can take place when

$$Re_L \approx \frac{1}{60^{1/3}} (g' L / u_*^2)^{1/3} < 2.74 \qquad (3)$$

where $g' = g\Delta\rho/\rho$ is the reduced gravity, $\Delta\rho$ the density difference across the leading edge of the plume, $\rho$ the water density, $u_*$ the frictional velocity in water, and the $L$ leading edge width (the distance to which the denser water propagates over the plume edge). For the case shown in Figure 6, $Re_L \approx 1$, which satisfies inequality (3). There are indeed indications of intense mixing on the upwind side of the plume (Figure 6), and this is consistent with theory. Note that freshwater plumes with a larger density difference and/or lower wind speed may not satisfy condition (3). This theory also ignores Coriolis forces and, strictly speaking, is valid only for the equatorial region.

## CONCLUSIONS

Convective rains within the ITCZ produce localized freshwater plumes, which tend to spread horizontally. These plumes resemble gravity currents and can interact with background stratification and wind stress. The dynamics of these near-surface plumes are inherently three dimensional, and explicit modeling of the processes

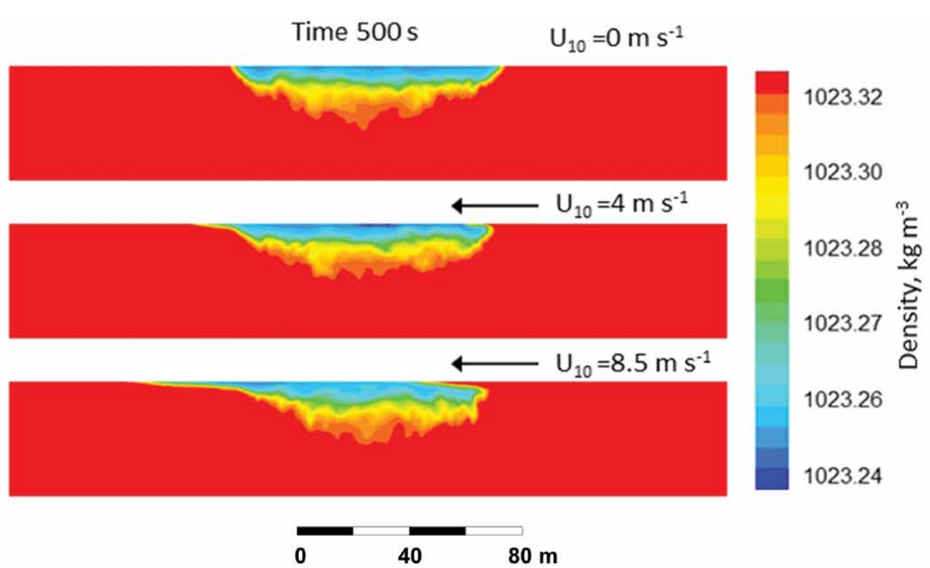


**FIGURE 4.** Contours of the near-surface freshwater plume interacting with wind stress (side view). The length scale is the same for both coordinates.

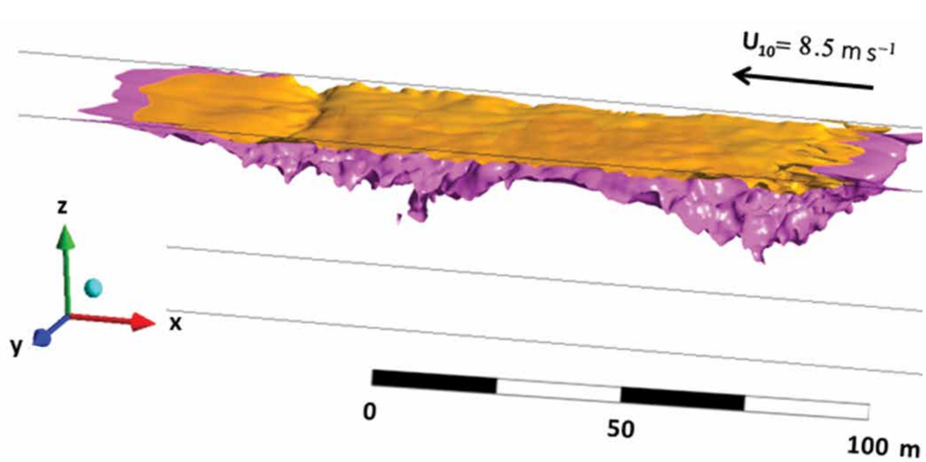


**FIGURE 5.** A bird's-eye view of the freshwater lens under wind stress action after a 1,000 s simulation contoured with salinity isosurfaces at 34.92 psu (brown) and 34.97 psu (pink). The length scale is the same for all three coordinates.

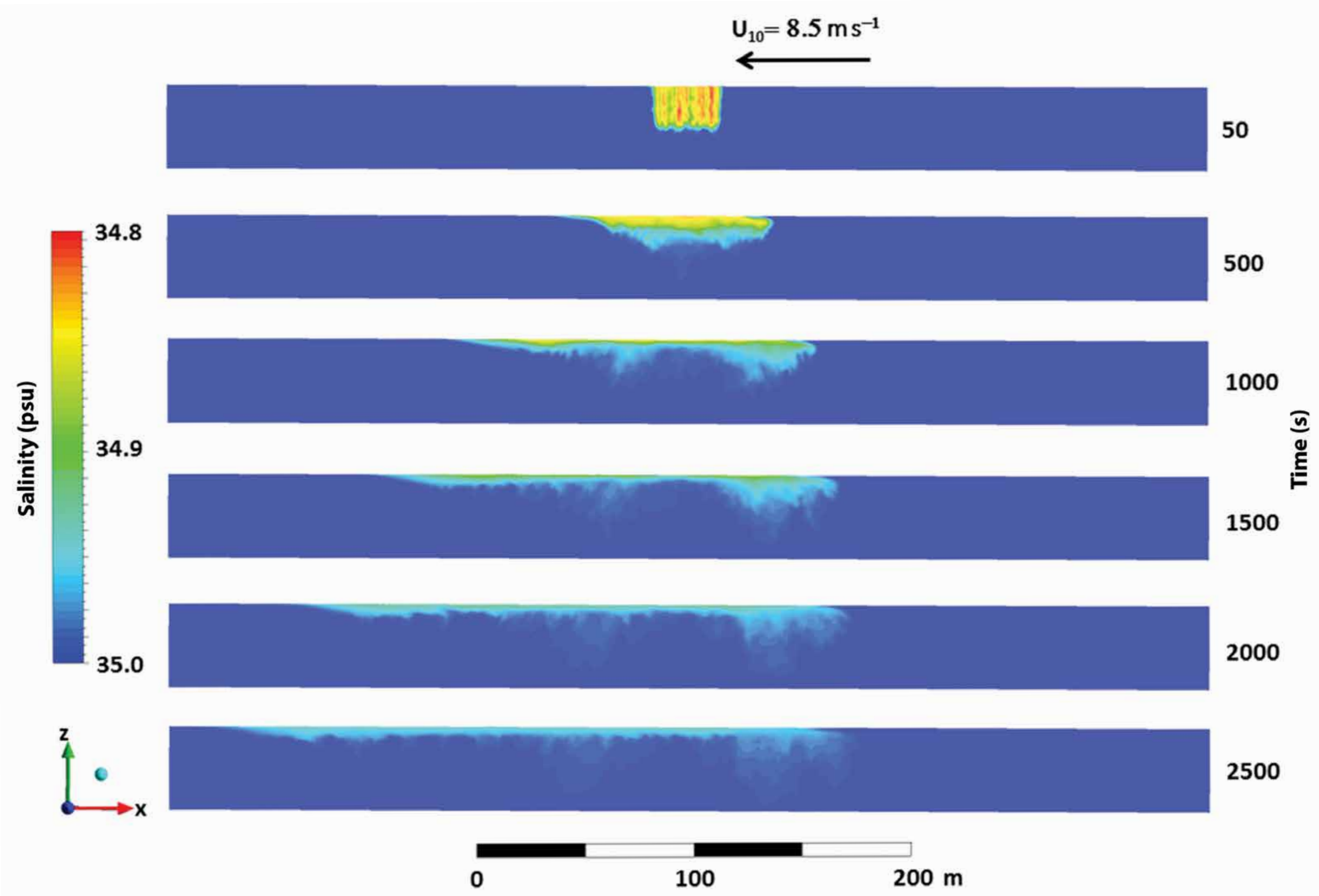


**FIGURE 6.** Evolution of the freshwater plume interacting with wind stress. The contour plot of salinity (side view) reveals strong asymmetry of the freshwater lens structure and mixing relative to wind direction. Note that the red color here corresponds to lower salinity. The length scale is the same for horizontal and vertical axes. A related animation is available in the online supplementary material at http://www.tos.org/oceanography/archive/28-1_soloviev.html.

involved requires high-resolution, non-hydrostatic three-dimensional models. In this work, we use computational fluid dynamics to reproduce the interaction of a freshwater lens with a stratified environment and wind stress. Our model reproduces development of coherent structures (streaks or rolls) in the propagating plume and resonant interaction between a near-surface freshwater plume and ambient stratification, which can lead to repeating frontal interfaces or "surface lines" that have been previously reported from field observations (Soloviev and Lukas, 1997). However, coherent streaks await detailed investigation.

Our results also indicate that wind stress interacting with a near-surface freshwater plume can lead to marked asymmetry in sea surface signature, propagation, and mixing associated with the plume. This is consistent with substantial

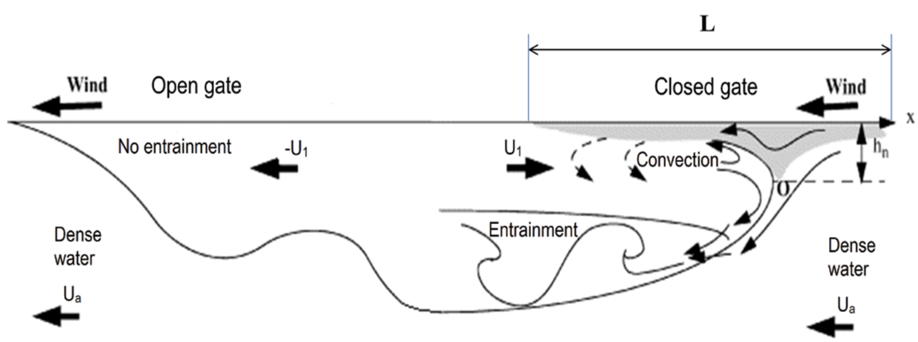


**FIGURE 7.** Depiction of Stommel's Overturning Gate in application to the near-surface freshwater plume propagating as the gravity current and interacting with wind stress, as proposed by Soloviev and Lukas (1997).

statistics collected during TOGA COARE (Soloviev et al., 2002).

One interesting result that can be useful for planning future fieldwork is that freshwater lenses spread rapidly horizontally and at the same time collapse vertically. This process results in the presence of shallow, low-salinity layers in the upper few meters of the ocean under low and moderate wind speed conditions. Soloviev and Lukas (1997) observed such shallow freshened layers during TOGA COARE. Apparently, the relationship between the vertical and horizontal structures of near-surface salinity fields depends on environmental conditions (wind and waves), and a full investigation is planned in the Pacific during SPURS-2. These processes potentially impact barrier layer physics and thus affect Aquarius and SMOS satellite image formation.

Influx of freshwater due to convective rains can result in substantial localized salinity anomalies (freshwater lenses) in the upper few meters of the ocean. The Aquarius and SMOS missions do not explicitly resolve fine surface salinity structures because the spatial resolution of these satellites is of the order of 100 km. Nevertheless, understanding the mixing and advection processes associated with freshwater lenses is important for calibration and correct interpretation of satellite salinity imagery (Farrar et al., 2014).

Future modeling work should investigate the dynamics of freshwater plumes under the influence of both ambient stratification and wind stress and how they interact to affect plume dynamics. The Coriolis force and temperature anomalies in the freshwater plume should be included in future models as well. Synthetic aperture radar data, which under certain conditions can resolve horizontal features on the sea surface associated with freshwater plumes down to the 1 m scale, should be useful for model verification (Matt et al., 2014).

**ONLINE SUPPLEMENT.** A related animation of the evolution of a freshwater plume interacting with wind stress is available in the online supplementary material at http://www.tos.org/oceanography/archive/28-1_soloviev.html.

**ACKNOWLEDGEMENTS.** We thank Mikhail Gilman (North Carolina State University) for development of user-defined functions for ANSYS Fluent software. Cayla Dean helped with numerical simulations and Bryan Hamilton (Nova Southeastern University) with manuscript arrangement. We are grateful to Lisan Yu (WHOI) for useful discussion of this work. The article was initiated as a follow up to the SPURS-2 Planning Meeting held April 16–18, 2014, in Pasadena, CA, attended by one of the authors (Soloviev). We acknowledge support from the Gulf of Mexico Research Initiative Consortium for Advanced Research on the Transport of Hydrocarbons in the Environment (PI: Tamay Özgökmen, UM). Silvia Matt has been supported by a National Research Council Research Associateship.

## REFERENCES

Anderson, J.E., and S.C. Riser. 2014. Near-surface variability of temperature and salinity in the near-tropical ocean: Observations from profiling floats. *Journal of Geophysical Research* 119:7,433–7,448, http://dx.doi.org/10.1002/2014JC010112.

Asher, W.E., A.T. Jessup, R. Branch, and D. Clark. 2014. Observations of rain-induced near surface salinity anomalies. *Journal of Geophysical Research: Oceans* 119(8):5,483–5,500, http://dx.doi.org/10.1002/2014JC009954.

Farrar, J.T., R. Schmitt, L. Rainville, W. Asher, B. Hodges, A. Jessup, F. Bingham, A. Shcherbina, W.S. Kessler, L. Centurioni, and others. 2014. *Report of a Workshop in Pasadena, April 16–18, 2014*. 17 pp.

Kuettner, J.P. 1971. Cloud bands in the earth's atmosphere: Observations and theory. *Tellus* 23(4–5):404–426.

Lesieur, M. 2008. *Turbulence in Fluids*, 4th ed. Springer, Berlin, Heidelberg, 558 pp.

Lukas, R., and E. Lindstrom. 1991. The mixed layer of the western equatorial Pacific Ocean. *Journal of Geophysical Research* 96(S01):3,343–3,357, http://dx.doi.org/10.1029/90JC01951.

Matt, S., A. A. Fujimura, Soloviev, and S. Rhee. 2011. Modification of turbulence air-sea interface due to the presence of surfactants and implications for gas exchange: Part II. Numerical simulations. Pp. 299–312 in *Gas Transfer at Water Surfaces*. Kyoto University Press.

Matt, S., A. Fujimura, A. Soloviev, S.H. Rhee, and R. Romeiser. 2014. Fine-scale features on the sea surface in SAR satellite imagery: Part II. Numerical modeling. *Ocean Science* 10:427–438, http://dx.doi.org/10.5194/os-10-427-2014.

Nicoud, F., and F. Ducros. 1999. Subgrid-scale stress modelling based on the square of the velocity gradient tensor. *Flow, Turbulence and Combustion* 62:183–200.

Özgökmen, T.M., P.F. Fischer, J. Duan, and T. Iliescu. 2004. Three-dimensional turbulent bottom density currents from a high-order nonhydrostatic spectral element model. *Journal of Physical Oceanography* 34:2,006–2,026, http://dx.doi.org/10.1175/1520-0485(2004)034<2006:TTBDCF>2.0.CO;2.

Simpson, J.E. 1987. *Gravity Currents: In the Environment and the Laboratory. Ambient Stratification.* Ellis Horwood Limited, NY, 186 pp.

Soloviev, A.V., and R. Lukas. 1997. Sharp frontal interfaces in near-surface layer of the ocean in the western equatorial Pacific warm pool. *Journal of Physical Oceanography* 27:999-1,017, http://dx.doi.org/10.1175/1520-0485(1997)027<0999:SFIITN>2.0.CO;2.

Soloviev, A.V., and R. Lukas. 2014. *The Near-Surface Layer of the Ocean: Structure, Dynamics, and Applications,* 2nd ed. Springer, NY, 552 pp.

Soloviev, A.V., R. Lukas, and H. Matsuura. 2002. Sharp frontal interfaces in the near-surface layer of the tropical ocean. *Journal of Marine Systems* 37(1–3):47–68, http://dx.doi.org/10.1016/S0924-7963(02)00195-1.

Stommel, H. 1993. A conjectural regulating mechanism for determining the thermohaline structure of the oceanic mixed layer. *Journal of Physical Oceanography* 23(1),142–148, http://dx.doi.org/10.1175/1520-0485(1993)023<0142:ACRMFD>2.0.CO;2.

Strelets, M. 2001. Detached eddy simulation of massively separated flows. AIAA 2001-0879, *39th AIAA Aerospace Sciences Meeting and Exhibit*, Reno, NV.

Vinayachandran, P.N., V.S.N. Murty, and V. Ramesh Babu. 2002. Observations of barrier layer formation in the Bay of Bengal during summer monsoon. *Journal of Geophysical Research* 107, http://dx.doi.org/10.1029/2001JC000831.

Wijesekera, H.W, C.A. Paulsom, and A. Huyer. 1999. The effect of rainfall on the sea surface layer during a westerly wind burst in the western equatorial Pacific. *Journal of Physical Oceanography* 29(4):612–632, http://dx.doi.org/10.1175/1520-0485(1999)029<0612:TEOROT>2.0.CO;2.

**AUTHORS. Alexander V. Soloviev** (soloviev@nova.edu) is Professor, Nova Southeastern University Oceanographic Center, Dania Beach, FL, USA, and Adjunct Professor, Rosenstiel School of Marine and Atmospheric Science, University of Miami, Miami, FL, USA. **Silvia Matt** is Oceanographer, Naval Research Laboratory, Stennis Space Center, MS, USA. **Atsushi Fujimura** is a graduate student at the Rosenstiel School of Marine and Atmospheric Science, University of Miami, Miami, FL, USA.

## ARTICLE CITATION

Soloviev, A.V., S. Matt, and A. Fujimura. 2015. Three-dimensional dynamics of freshwater lenses in the ocean's near-surface layer. *Oceanography* 28(1):142–149, http://dx.doi.org/10.5670/oceanog.2015.14.